ジルコニア微粉末の焼結挙動に及ぼす添加物の効果：アルミナとシリカ添加の比較

松　井　光　二

Effects of additives on sintering behavior of fine zirconia powder : comparison between alumina and silica additions

Koji MATSUI

The sintering behavior of 3 mol% Y_2O_3-doped ZrO_2 powders with and without a small amount of Al_2O_3 or SiO_2 was investigated to clarify the difference in the effects of their additives on the initial sintering stage. The shrinkage behavior of powder compact was measured under constant rates of heating (CRH). The sintering rate remarkably increased by a small amount of Al_2O_3 or SiO_2 addition, and the enhanced sintering effect by Al_2O_3 addition was greater than that by SiO_2 one. The apparent activation energy (nQ) and apparent frequency factor (β_0^g), where the n is the order depending on diffusion mechanism, were estimated at the initial sintering stage by applying the sintering-rate equation to the CRH data. The diffusion mechanism changed from grain-boundary diffusion to volume diffusions by Al_2O_3 or SiO_2 addition. Both nQ and β_0^g increased in the order of Al_2O_3 > SiO_2 > no additions. It is, therefore, concluded that the sintering rate increases in the order of Al_2O_3 > SiO_2 > no additions because the increase in β_0^g rather than nQ is predominant.

1. Introduction

Due to its excellent mechanical properties (i.e., high strength and fracture toughness), Y_2O_3-stabilized tetragonal ZrO_2 polycrystal (Y-TZP) has become an important structural ceramic, finding use in optical fiber connectors, grinding media, and precision parts. The mechanical properties strongly depend on the microstructure in Y-TZP, which can be controlled by applying the sintering-acceleration effect of additive. The appearance of high-performance Y-TZP for new application is desired to spread the zirconia-product market. To develop high-performance Y-TZP powder, it is needed to clarify the effect of various additives on the sintering mechanism of Y-TZP powder.

The initial sintering mechanism of various ceramic powders has been investigated extensively.[1)-14)] For instance, Young and Cutler[1)] have derived sintering-rate equations that is applicable to shrinkage data measured under constant rates of heating (CRH), and estimated the activation energy for causing diffusion at the initial sintering stage in Y_2O_3-stabilized ZrO_2. Wang and Raj[2), 3)] have investigated the densification behavior in Al_2O_3, ZrO_2/Al_2O_3 composite, and ZrO_2 containing Y_2O_3 by the CRH method. Thus far, the author has kinetically investigated the initial sintering mechanism in Y_2O_3-doped ZrO_2 powders with and without 0.25 mass% Al_2O_3, and clarified the following points.[4)-8)]

i) Al_2O_3 effect: Al_2O_3 changes the diffusion mechanism from grain-boundary (GBD) to volume diffusions (VD) at the initial sintering stage.[4)-6)] As a result, the densification is enhanced because the apparent frequency-factor term in the rate constant increases.[6)]

ii) Specific surface-area effect: when the specific surface area in Y_2O_3-doped ZrO_2 powder increases,

the sintering rate is enhanced because of an increase in frequency-factor term.[7]

iii) Y_2O_3 concentration effect: the increase in Y_2O_3 concentration decreases the sintering rate because of increasing the activation energy of diffusion.[8]

Furthermore, the author also proposed an analytical method that can experimentally determine the diffusion mechanism at the initial sintering stage using CRH data, and demonstrated the validity of the analytical method using Y_2O_3-doped ZrO_2 powders with and without 0.25 mass% Al_2O_3.[4),5)]

From the industrial standpoint, it is important to clarify the roles of various additives which accelerate sintering in Y-TZP. Usually, not only Al_2O_3 but also SiO_2 is well used as one of the additives. As described in the above-mentioned, the effect of Al_2O_3 on the initial sintering stage in Y-TZP powder has been reported in previous papers.[4),6)-8)] For the effect of SiO_2, the superplasticity behavior and microstructure development in SiO_2-doped Y-TZP has been investigated previously.[15)-18)] However, the effect of SiO_2 addition on the initial sintering stage of Y-TZP powder has not been reported in the previous papers. Furthermore, although Al_2O_3 and SiO_2 are well used as additives which enhance the sintering rate in Y-TZP powder, the difference in their effects is not quantitatively discussed.

In the present study, Al_2O_3 and SiO_2 as additives were noted, and the initial sintering behavior of Y-TZP powders with and without Al_2O_3 or SiO_2 was analyzed by the CRH method. The difference in the enhanced sintering effect of these additives was quantitatively discussed based on the present analytical results.

2. Experimental procedure

[1] Specimen preparation

3 mol% (5.2 mass%) Y-TZP powder with a specific surface area of 15 m^2/g (TZ-3Y grade, Tosoh, Tokyo, Japan), colloidal SiO_2 (Snowtex, Nissan Chemical Industries, Tokyo, Japan) with a particle size in the range of 10-20 nm, and fine Al_2O_3 powder (Alu C grade, Tokyo, Nippon Aerosil, Japan) with a specific surface area of *ca.* 100 m^2/g were used as starting materials. The Y-TZP powder with 0.25 mass% Al_2O_3 (3YA) or SiO_2 (3YC) was prepared by wet-milling the Y-TZP powder and colloidal SiO_2 or Al_2O_3 powder with a vibration mill. The atomic ratios of Al/(Zr+Y) and Si/(Zr+Y) of these powders are 6×10^{-3} and 5×10^{-3}, respectively, which are roughly equal. For comparison with the sintering behavior of 3YA and 3YC, the Y-TZP powder without Al_2O_3 or SiO_2 (3Y) was also treated by wet-milling under the same process.

These powders were pressed uniaxially into a disk under 70 MPa. The powder compacts were *ca.* 25mm∅ ×4mm in size, and sintered at 1100 °-1500℃ for 2 h in air (heating rate 100℃/h).

[2] Density and grain-size measurements

The density of sintered bodies was measured using the Archimedes method for the relative densities of ≥ 80 %, whereas calculated from the weight and the size for the relative densities of < 80 %. A scanning electron microscopy (SEM; Model S-4500, Hitachi, Tokyo, Japan) was used to observe the microstructure and estimate the average grain sizes of sintered bodies. SEM specimens were polished with a diamond paste of 3 μm, and then thermally etched in air for 1 h at a 50℃ lower temperature than the sintering temperature of each specimen. The average grain size was measured by the Planimetric method.[19)]

[3] CRH measurements

The powders were pressed uniaxially into a cylindrical disk under *ca.* 100 MPa and afterwards pressed isostatically at 200 MPa by cold isostatic pressing. The specimen was 6 mm∅ ×15 mm. The shrinkage of the powder compacts obtained with sintering was measured using a dilatometer (Model DL 9700, ULVAC-RIKO, Yokohama, Japan). The shrinkage measurements by the CRH technique were performed in the range from room temperature to 1500℃ at heating rates of 5 °, 10 °, 15 °, and 20℃/min in air. When the temperature reached 1500℃, the specimens were cooled at a constant rate. The dilatometer was calibrated using sapphire as a standard specimen. Thermal expansion of each specimen was corrected by the same method in the previous paper.[4)] It was confirmed that the shrinkage proceeded isotropically because for each measured specimen, the shrinkage percentage of length axis was nearly equal to that of diameter axis. Assuming isotropic shrinkage to powder

compact, the density ρ(T) at a given temperature T is given by the following equation[2]:

$$\rho(T)=\left(\frac{L_f}{L(T)}\right)^3\rho_f \quad (1)$$

where L_f and $L(T)$ are the final length and the length at a T of the specimen, respectively. ρ_f indicates the final density measured by the Archimedes method. The $\rho(T)$ at a T was calculated using Eq. (1).

[4] Analysis of initial sintering mechanism

The material-transport path and activation energy of diffusion at the initial sintering stage were determined by the same analytical method as the previous paper.[5] The sintering-rate equation at the initial sintering stage is given by the following equation[9]:

$$\frac{d}{dt}\left[\left(\frac{\Delta L}{L_0}\right)^{1/n}\right]=\frac{K\gamma_s\Omega D}{kTa^p} \quad (2)$$

where $\Delta L(=L_0-L)$ is the change in length of the specimen, L_0 the initial length of the specimen, K the numerical constant, γ_S the surface energy, Ω the atomic volume, D the diffusion coefficient, t the time, T absolute temperature, k the Boltzmann's constant, a the particle radius, and the parameters of n and p the order depending on the diffusion mechanism. The values of p for GBD and VD are 4 and 3, respectively. The value of K includes the effective grain-boundary width in GBD.[10] Equation (2) is applicable to the fractional shrinkages of < 4% that satisfy the initial sintering condition.

The following sintering-rate equation that is applicable to CRH data is derived from Eq. (2).[5]

$$\ln\left[T\left(\frac{dT}{dt}\right)\left(\frac{d\rho}{dT}\right)\right]=-\frac{Q}{RT}+\alpha(n,p) \quad (3)$$

where

$$\alpha(n,p)=\ln[f(\rho,n)]+\ln\left[\frac{K\gamma_s\Omega D_0}{k}\right]-p\ln a \quad (4)$$

Here, Q is the activation energy, R the gas constant, $f(\rho, n)$ the density function that depends on the n, and D_0 the pre-exponential term defined as $D=D_0\exp(-Q/RT)$. Equation (3) corresponds to the sintering-rate equation derived by Wang and Raj.[2] Using the slope S_1 of the Arrhenius-type plot of $\ln[T(dT/dt)(d\rho/dT)]$ against $1/T$ at the same density, the Q is expressed as

$$Q=-RS_1 \quad (5)$$

On the other hand, the following sintering-rate equation that is different from the type of Eq. (3) is also derived from Eq. (2).[5]

$$\frac{d(\Delta L/L_0)}{dT}=\left(\frac{K\gamma_s\Omega D_0R}{ka^pcQ}\right)^n\cdot\left(\frac{nQ}{RT^{2-n}}\right)\cdot\exp\left(-\frac{nQ}{RT}\right) \quad (6)$$

Here, c is the heating rate (i.e., $c=dT/dt$). For $n=1/3$ and $n=1/2$, Eq. (6) corresponds to the sintering equations derived by Young and Cutler.[1] This rate equation is also applied to CRH data. Using the slope S_2 of the Arrhenius-type plot of $\ln[T^{2-n}d(\Delta L/L_0)/dT]$ against $1/T$, the apparent activation energy (nQ) is expressed as

$$nQ=-RS_2 \quad (7)$$

Here, the n is in the range of 0.31-0.50.[10] In the previous paper, the author has reported that the values of nQ in 3 mol % (5.3 mass%) Y-TZP powder with a specific surface area of 6.7 m^2/g determined from Arrhenius-type plots that correspond to $n=1/3(=0.33)$ and $n=1/2(=0.50)$ were 219 and 217 kJ/mol, respectively.[4] This result suggests that the nQ is nearly the same value in the n range of 0.31-0.50. Therefore, the S_2 can be estimated as the approximate value from the Arrhenius-type plot of $\ln[T^{1.6}d(\Delta L/L_0)/dT]$ against $1/T$ that corresponds to $n=0.4$ that is the central value of $n=0.31$-0.50.[5] Combining Eqs.(5) and (7), the following equation is obtained[5]:

$$n=\frac{nQ}{Q}=\frac{S_2}{S_1} \quad (8)$$

In the present analysis, the Q and n were determined in the fractional shrinkage range of <4 % that satisfies the initial sintering condition as with previous papers.[4),5)] In previous papers, the author analyzed the isothermal shrinkage behavior of Y-TZP powders with and without a small amount of Al_2O_3, and showed that the logarithm shrinkage-logarithm time (log-log) plots in the shrinkage range of < 4% measured at various constant temperatures became the linear relationships.[6)-8)] At the initial sintering process with particle growth, it has been reported that the log-log plot show no linear relationship.[11)] Therefore, the influence of particle growth on the Q and nQ is negligibly small in the shrinkage range of < 4 %.

3. Results

[1] Densification and grain growth

Figure 1 shows the change of relative density in 3Y

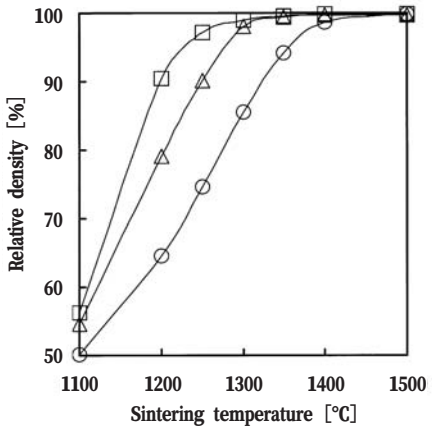

Fig. 1 Changes of relative density and average grain size in 3Y, 3YA, and 3YC with sintering temperature. The duration time at each sintering temperature is 2 h. (○), (□), and (△) indicate 3Y, 3YA, and 3YC, respectively.

(without additive), 3YA (with 0.25 mass% Al_2O_3), and 3YC (with 0.25 mass% SiO_2) with sintering temperature. The relative density of 3YC was higher than that of 3Y at lower temperatures. The relative density of 3YA was higher than that of 3YC at lower temperatures, and attained 99.5 % at 1350℃. This result reveals that the densification of Y-TZP powder is accelerated by Al_2O_3 or SiO_2 addition, and the acceleration effect by Al_2O_3 addition is greater than that by SiO_2 one. Figure 2 shows SEM images of the polished and etched surfaces of 3Y, 3YA, and 3YC sintered at 1500℃. The average grain sizes of 3Y, 3YA, and 3YC were nearly equal, and in the range of 0.5–0.6 μm. This result suggests that at the sintering-hold time of 2h, the effect of Al_2O_3 or SiO_2 addition did not appear for the grain-growth process.

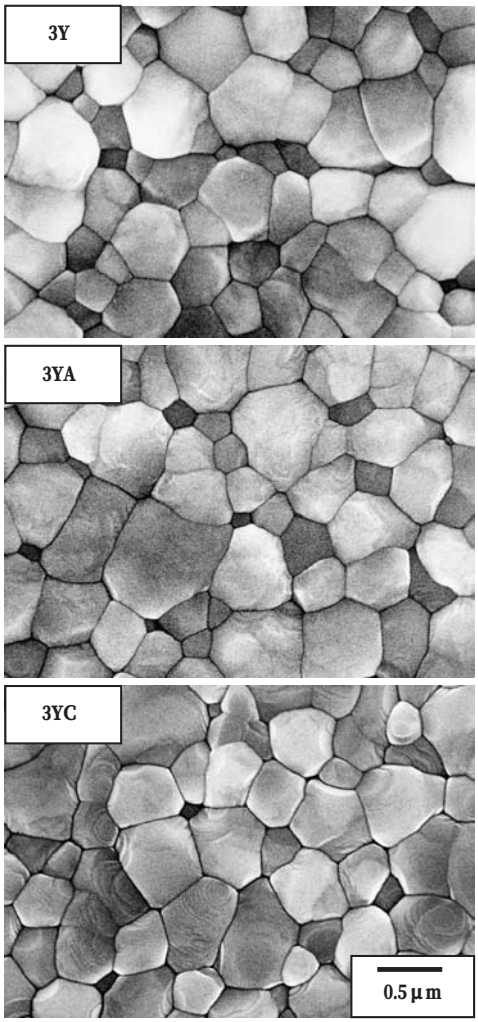

Fig. 2 Scanning electron microscopy images of 3Y, 3YA, and 3YC sintered at 1500℃. The duration time at each sintering temperature is 2 h.

[2] Densification behavior

Figure 3 shows the changes of the shrinkage of 3Y, 3YA, and 3YC with temperature in the course of 10℃/min heating. As can be seen in **Fig. 3**(a), the starting

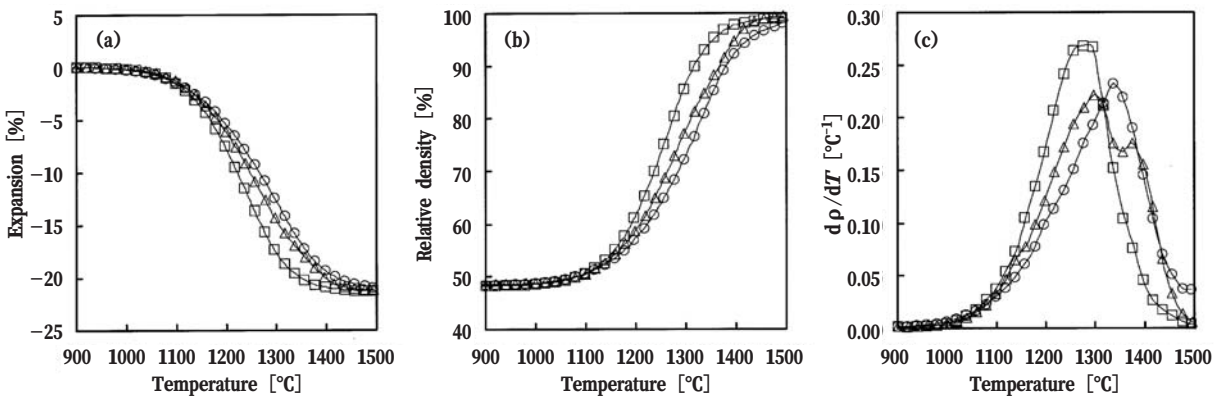

Fig. 3 Temperature dependence of shrinkage, relative density (ρ), and densification rate (dρ/dT) of 3Y, 3YA, and 3YC in the course of heating (10℃/min). (○), (□), and (△) indicate 3Y, 3YA, and 3YC, respectively.

temperature of 3Y, 3YA, and 3YC is nearly equal, and the shrinkage increased in the order of 3YA > 3YC > 3Y at temperatures of > ～1100℃. Using the shrinkage curves in **Fig.3**(a), the temperature changes of the relative density (ρ) and the densification rate ($d\rho/dT$) were determined by Eq.(1) (Figs.3(b) and (c)). The ρ was high in the order of 3YA > 3YC > 3Y at temperatures of > ～1100℃. The $d\rho/dT$ increased in the order of 3YA > 3YC > 3Y when the temperature exceeded ～1100℃, and the temperature of peak maximum of the $d\rho/dT$ curve became low in the order of 3YA < 3YC < 3Y. The heating-rate dependence of $d\rho/dT$ in each specimen was also examined in the range of 5 °-20℃/min. For all specimens, the $d\rho/dT$ curves shifted to a higher temperature, as the heating rate increased. As an example, the heating-rate dependence of 3YC is shown in **Fig. 4**. The present results reveal that Al_2O_3 or SiO_2 addition enhances the $d\rho/dT$, and the enhanced effect by Al_2O_3 addition is greater than that by SiO_2 one.

[3] CRH shrinkage analysis

In previous papers, the author reported the initial sintering mechanisms in Y-TZP powders with and without 0.25 mass% Al_2O_3.[4),6)-8)] However, the initial sintering mechanism of 3YC (with 0.25 mass% SiO_2) has not been reported previously. Therefore, the initial sintering behavior of 3YC is analyzed to clarify the difference between the sintering-acceleration effects by Al_2O_3 and SiO_2 additions. The Q, nQ, and n of diffusion at the initial sintering stage in 3YC can be estimated by applying Eqs. (3), (6), and (8) to the results in Figs. 3 and 4. Equation (3) is applied in the following way. For each heating rate (dT/dt), both T and $d\rho/dT$ at the same ρ were determined, and their values were plotted as $T(dT/dt)(d\rho/dT)$ against $1/T$ (**Fig. 5**). Here, this analysis was performed in the ρ range of ≤ 54 % that corresponds to the fractional shrinkage range of < 4 %. The plot at each ρ showed the linear relation because the values of correlation coefficient were in the range of -0.95 to -1.0. The Q at each ρ was determined from the slope of the straight line (**Fig. 6**). The average

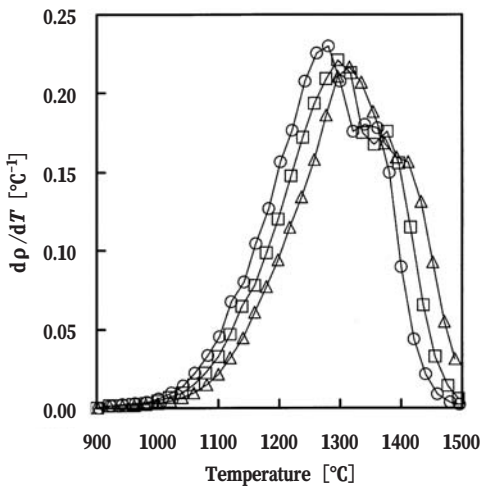

Fig. 4 Temperature dependence of densification rate ($d\rho/dT$) of 3YC at various heating rates. (○), (□), and (△) represent 5 °, 10 °, and 20℃/min heating rates. The data measured at a 15℃/min heating rate were also obtained in a similar manner.

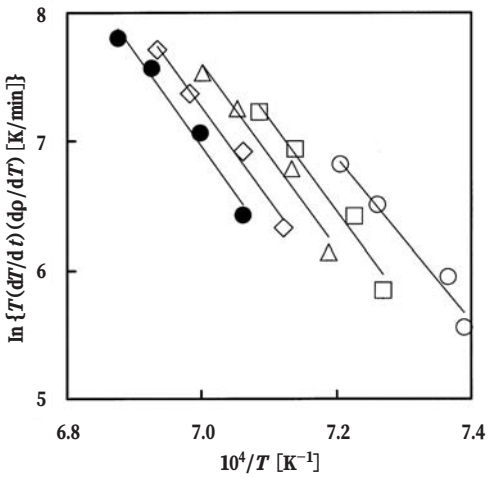

Fig. 5 Arrhenius-type plots of 3YC for the estimate of activation energies of sintering. (○), (□), (△), (◇), and (●) represent 50%, 51%, 52%, 53%, and 54% relative densities, respectively. The data of 50.5%, 51.5%, 52.5%, and 53.5% relative densities were also obtained in a similar manner.

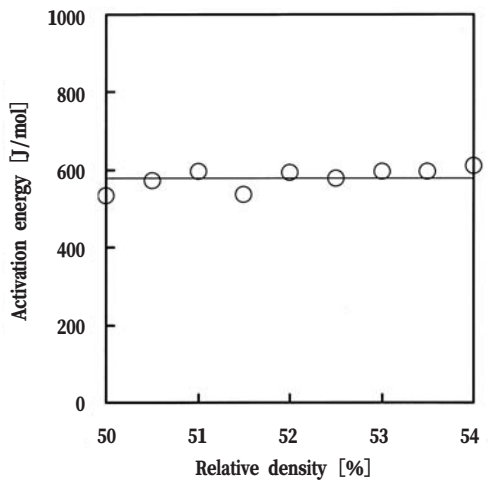

Fig. 6 Activation energies for diffusion of 3YC in the relative density of 50-54%.

value of Q in this ρ range was 579 kJ/mol (standard deviation (σ)=28 kJ/mol). On the other hand, Eq. (6) is applied in the following way. In the fractional shrinkage range of <4 %, the nQ was determined from the slope of the straight line in the plot of $\ln[T^{1.6}\mathrm{d}(\Delta L/L_0)/\mathrm{d}T]$ against $1/T$ using the shrinkage curve of each $\mathrm{d}T/\mathrm{d}t$. As an example, the plot at a $\mathrm{d}T/\mathrm{d}t$ of 10°C/min is shown in **Fig.5**. It is seen that the plot shows the linear relation. The linear relations were obtained at all plots of 5-20°C/min heating rates. Determining the average value of nQ, 280 kJ/mol (σ=6 kJ/mol) was obtained. Using the average values of both Q and nQ, the n was determined by Eq. (8), which was n=0.5(=1/2). According to two-sphere shrinkage models, the n ranges of GBD and VD are 0.31-0.33 and 0.40-0.50, respectively.[10] Therefore, the diffusion mechanism of 3YC was assigned to VD. This diffusion mechanism (i.e., n=1/2) agreed with that of Al_2O_3 addition in previous papers.[4)-8)]

To clarify the difference between Al_2O_3 and SiO_2 effects on the sintering rate, the Q and frequency factor (that is defined by the following β_0) of each specimen are estimated using Eq. (6). Putting as $\beta_0=(K\gamma_S\Omega D_0)/(ka^p)$, Eq. (6) is expressed by

$$\frac{\mathrm{d}(\Delta L/L_0)}{\mathrm{d}T}=\beta_0^n\cdot\left(\frac{R}{cQ}\right)^n\cdot\left(\frac{nQ}{RT^{2-n}}\right)\cdot\exp\left(-\frac{nQ}{RT}\right) \quad (9)$$

In previous papers, the author reported that the orders depending on the diffusion mechanism of Y-TZP powder with and without 0.25 mass% Al_2O_3 were n=1/2 and n=1/3, respectively,[4),6-8)] which can be applied as the orders for 3Y and 3YA. In the above result, the order of 3YC is n=1/2. Using each value of n, Eq. (9), and the shrinkage data (of < 4 %) of 5-20°C/min heating rates, the average values of Q were determined from the slopes of the straight lines in the plots of $\ln[T^{5/3}\mathrm{d}(\Delta L/L_0)/\mathrm{d}T]$ against $1/T$ for 3Y (n=1/3) and $\ln[T^{3/2}\mathrm{d}(\Delta L/L_0)/\mathrm{d}T]$ against $1/T$ for 3YA and 3YC (n=1/2). Each β_0 was determined from the intercept of the plot using the determined Q. As an example, each plot at a 10°C/min heating rate is shown in **Fig. 8**. Here, although the Q of 3YC has been already determined from the result in **Fig. 6**, it was re-estimated using Eq. (9) to strictly comparable with Qs of 3Y and 3YA. The obtained results are shown in **Table 1**. The Q increased in the order of 3Y > 3YA > 3YC. Similarly, the β_0 also increased in the order of 3Y > 3YA > 3YC. In previous papers, the author determined

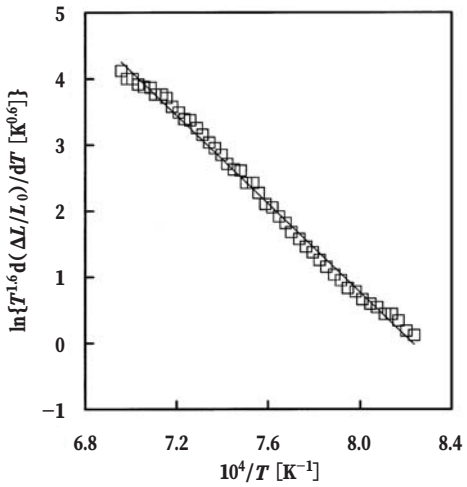

Fig. 7 Plot of $\ln[T^{1.6}\mathrm{d}(\Delta L/L_0)/\mathrm{d}T]$ against $1/T$ of 3YC in the course of heating (10°C/min).

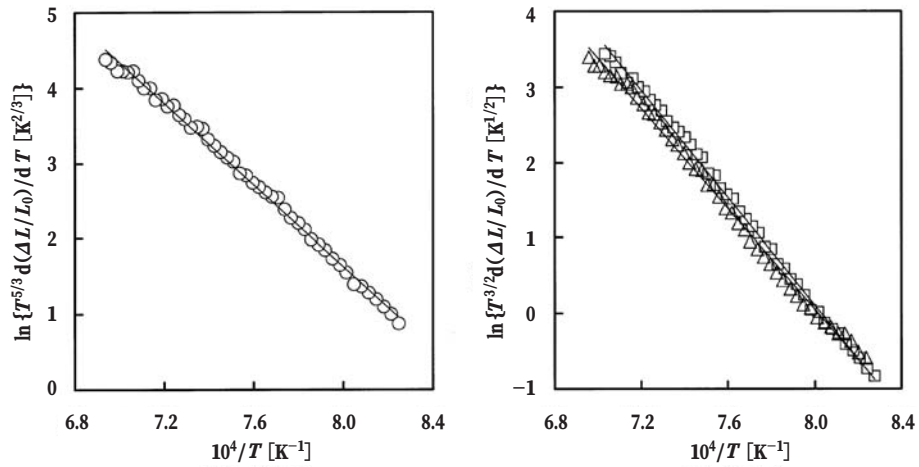

Fig. 8 Plots of $\ln[T^{5/3}\mathrm{d}(\Delta L/L_0)/\mathrm{d}T]$ against $1/T$ in 3Y and $\ln[T^{3/2}\mathrm{d}(\Delta L/L_0)/\mathrm{d}T]$ against $1/T$ in 3YC in the course of heating (10°C/min). (○), (□), and (△) indicate 3Y, 3YA, and 3YC, respectively.

Table I　Apparent activation energies, apparent frequency factors, activation energies, and frequency factors for diffusion at initial sintering stage

Specimen	Activation energy*		Frequency factor*		Apparent activation energy		Apparent frequenecy factor	
	Q (kJ/mol)	Standard deviation	$\ln[\beta_0, (s^{-1})]$	Standard deviation	nQ (kJ/mol)	Standard deviation	$\ln[\beta_0^n, (s^{-n})]$	Standard deviation
3Y	681	17	51.4	1.5	227	6	17.1	0.5
3YA	589	7	46.1	0.6	295	4	23.0	0.3
3YC	558	13	43.0	1.1	279	6	21.5	0.5

* The values of Q and $\ln\beta_0$ were calculated from the values of nQ and $\ln\beta_0^n$ using n=1/3 for 3Y and n=1/2 for 3YA and 3YC.

the values of Q for sintering of 3 mol% (5.1–5.3 mass%) Y-TZP powders by the CRH and isothermal shrinkage analyses to be 535–595 with 0.25 mass% Al_2O_3 and 647–694 kJ/mol without Al_2O_3.[4),6-8)] Furthermore, the author also reported that the values of $\ln[\beta_0, (s^{-1})]$ of 3Y and 3YA determined by the isothermal shrinkage analysis were 48.2 and 45.7, respectively.[6),8)] Compared with these values, the values of Q and β_0 in 3Y, 3YA, and 3YC determined by the present analytical method are considered to be reasonable. It is, therefore, clarified that the difference in the sintering rate by Al_2O_3 and SiO_2 additions occurs by differences in both Q and β_0 at the initial sintering stage.

4. Discussion

[1] Effects of additives on the sintering rates

Based on the kinetic analysis, the effects of Al_2O_3 and SiO_2 additions on the initial sintering stage are discussed as follows. The integral type of Eq. (6) is given by the following equation.[5)]

$$\left(\frac{\Delta L}{L_0}\right)=\left(\frac{K\gamma_s\Omega D_0 R}{ka^p cQ}\right)^n T^n \exp\left(-\frac{nQ}{RT}\right) = \beta_0^n\left(\frac{RT}{cQ}\right)^n \exp\left(-\frac{nQ}{RT}\right) \quad (10)$$

Under the same diffusion mechanism (namely, a constant n), the decrease in β_0 under a constant Q and T or the increase in Q under a constant β_0 and T leads to the decrease in the $\Delta L/L_0$, which corresponds to the decrease in the sintering rate. As shown in **Fig. 3**, the shrinkage, ρ, and $d\rho/dT$ of 3YA were greater than that of 3YC when the temperature exceeded ～1100℃. As can be seen the result in **Table I**, both Q and β_0 of 3YA are greater than those of 3YC. It is, therefore, concluded that the sintering rate of 3YA increases more than that of 3YC at temperatures of ＞～1100℃ because the increase in β_0 rather than Q is predominant.

According to Eq. (10), the magnitude of n should be considered when the diffusion mechanism changes. The nQ and apparent frequency factor (β_0^n) were determined using the above Q and β_0, respectively (**Table I**). Both nQ and β_0^n increase in the order of 3YA ＞ 3YC ＞ 3Y. As can be seen from the result in **Fig. 3**, when the temperature exceeded ～1100℃, the sintering rate increases in the order of 3YA ＞ 3YC ＞ 3Y. It is, therefore, concluded that the sintering rate increases in the order of 3YA ＞ 3YC ＞ 3Y at temperatures of ＞～1100℃ because the increase in β_0^n rather than nQ is predominant. Thus, the sintering rate is controlled by not only the Q and β_0 but also the n.

[2] Mechanism of GBD→VD change by additive

In the previous paper, the author reported that the mechanism of GBD→VD change by Al_2O_3 addition is reasonably explained as follows.[6)] Added Al_2O_3 particles begin to dissolve in Y-TZP particles with neck formation and growth, and a part of the dissolved Al^{3+} ions segregates at grain boundaries formed between Y-TZP particles. When Al^{3+} ions segregate at grain boundaries, the grain-boundary energy (γ_{GB}) decreases, which is led to the change of diffusion mechanism from GBD to VD.

The similar discussion is available for the GBD→VD change by SiO_2 addition. Ikuhara *et al.*[15)] have reported that the dynamic behavior with heating of 2.5 mol% Y-TZP particles (Tosoh) to which SiO_2 particles with the diameter of 10 nm (Nissan Chemical Industries) was added was observed using *in-situ* observation technique by a transmission electron microscopy, and most of the SiO_2 particles in the mixed state were adsorbed into the ZrO_2 grains at ～1300℃. Furthermore, they showed that no amorphous layer exists along the grain-boundary faces in SiO_2-doped Y-TZP, but Y^{3+} and Si^{4+} ions segregate at grain boundaries over widths

of 4–6 and 5–8 nm, respectively.[16] Taking into account their observations,[15),16)] it is presumed that added SiO_2 particles begin to dissolve in Y-TZP particles with neck formation and growth, dissolved Si^{4+} ions diffuse to Y-TZP particle interior within the range of solubility, and a part of the dissolved Si^{4+} ions segregate at grain boundaries formed between Y-TZP particles. In the result in **Fig. 1**, a part of added SiO_2 has already dissolved in ZrO_2 particles at the temperature of ~ 1100℃, which is consistent with their result.[15] Furthermore, it has been reported that when Si^{4+} ions segregate at grain boundaries in 2.5 mol% Y-TZP, the γ_{GB}/γ_S relatively decreases.[20] It is, therefore, concluded that the diffusion mechanism changes from GBD to VD because the γ_{GB} decreases by the grain-boundary segregation of Si^{4+} ions.

[3] Effects of additives on the activation energy and frequency factor

Sakka *et al.* have reported that the cation diffusion in the Y_2O_3- and CeO_2-$(Zr_{1-x}Hf_x)O_2$ systems is much smaller than the oxygen diffusion.[21),22)] Therefore, the sintering rate in Y-TZP powders with and without a small amount of additive is controlled by the cation diffusion. In the previous paper, the author reported that the differences in both Q and β_0 between 3Y and 3YA (i.e., Q(3Y)>Q(3YA) and β_0(3Y)>β_0(3YA)) can be explained by the grain-boundary segregation of Y^{3+} ions and the difference in cation-vacancy (V_{Zr}'''') concentrations between grain-boundary vicinity and particle interior.[6] The difference in Q of VD between 3YA and 3YC (i.e., Q(3YA)>Q(3YC)) is discussed as follows. When Al_2O_3 dissolves to Y-TZP, the oxygen vacancy ($V_O^{\bullet\bullet}$) is produced by the doping reaction in the following equation.

$$Al_2O_3 + 2Zr_{Zr}^{\times} + O_O^{\times} \xrightarrow{ZrO_2} 2Al_{Zr}' + V_O^{\bullet\bullet} + 2ZrO_2 \quad (11)$$

On the other hand, when SiO_2 dissolves to Y-TZP, the $V_O^{\bullet\bullet}$ is not produced as shown in the following doping-reaction equation.

$$SiO_2 + Zr_{Zr}^{\times} \xrightarrow{ZrO_2} Si_{Zr}^{\times} + ZrO_2 \quad (12)$$

The cation diffusion proceeds primarily through cation vacancies (V_{Zr}'''') of the schottky-defect type. The formation of schottky defect is expressed by the following equilibrium reaction.

$$null = V_{Zr}'''' + 2V_O^{\bullet\bullet} \quad (13)$$

This equilibrium reaction means that when the $V_O^{\bullet\bullet}$ concentration increases, the V_{Zr}'''' concentration decreases according to the law of mass action. Furthermore, when the $V_O^{\bullet\bullet}$ concentration increases, because $V_O^{\bullet\bullet}$ associates with V_{Zr}'''' owing to coulombic attractive force, this associated V_{Zr}'''' does not work for the cation diffusion. The decrease in V_{Zr}'''' concentration and the association between V_{Zr}'''' and $V_O^{\bullet\bullet}$ retard the cation diffusion. When Al_2O_3 dissolves to Y-TZP, the cation diffusion is depressed because the $V_O^{\bullet\bullet}$ produces, and the depressing effect appears as the increase in the Q of VD. The dissolution of SiO_2 to Y-TZP hardly influences the cation diffusion because the $V_O^{\bullet\bullet}$ does not produce. Therefore, the Q of VD in Al_2O_3 addition is larger than that in SiO_2 one. The present results reveal that the Q of VD in 3YA is higher than that in 3YC (**Table I**), which is consistent with the conclusion in the above discussion. Therefore, the Q difference of VD between 3YA and 3YC can be qualitatively interpreted by the difference in the amount of $V_O^{\bullet\bullet}$ that is produced by the segregated dissolution of Al_2O_3 or SiO_2 at Y-TZP grain boundaries.

The difference in β_0 of VD between 3YA and 3YC (i.e., β_0(3YA)>β_0(3YC)) is discussed as follows. According to the random walk theory, the D_0 in the extrinsic region is given by the following equation.[23]

$$D_0 = \frac{1}{6} B\nu\lambda^2 N_V \exp\left(\frac{\Delta S^{\neq}}{R}\right) \quad (14)$$

Here, B is the constant that depends on the crystal structure, ν the frequency of atom, λ the space between crystal planes, N_V the vacancy concentration, and $\Delta S^{\neq}$ the activation entropy. When the diffusion mechanism changes from GBD to VD by dissolution of Al_2O_3, the V_{Zr}'''' concentration decreases (i.e., the decrease in N_V) because the $V_O^{\bullet\bullet}$ is formed. On the other hand, the formation of $V_O^{\bullet\bullet}$ causes the increase in γ_S.[6] In the case of SiO_2 addition, the V_{Zr}'''' concentration does not change and the γ_S change is small in comparison with Al_2O_3 addition because the $V_O^{\bullet\bullet}$ is not produced by the doping reaction of SiO_2. Substituting Eq. (14) into $\beta_0 = (K\gamma_S\Omega D_0)/(ka^P)$ and then taking β_0(3YA)/β_0(3YC), one obtains

$$\frac{\beta_0(3YA)}{\beta_0(3YC)} \cong \left(\frac{\gamma_s(3YA)}{\gamma_s(3YC)}\right)\left(\frac{N_v(3YA)}{N_v(3YC)}\right) \quad (15)$$

Here, it is presumed that K, Ω, B, ν, λ, and ΔS^{*} do not vary by the difference in Al_2O_3 and SiO_2 additions. The β_0 of VD in 3YA is higher than that of VD in 3YC (i.e., $\beta_0(3YA)/\beta_0(3YC)>1$). The right side in Eq. (15) is the relations of $\gamma_S(3YA)/\gamma_S(3YC)>1$ and $N_V(3YA)/N_V(3YC)<1$. It is, therefore, concluded that the β_0 in 3YA becomes higher than that in 3YC because the increase in γ_S rather than the decrease in N_V by Al_2O_3 addition is predominant.

As discussed in Section IV. (1), the increase of sintering rate by Al_2O_3 or SiO_2 addition largely depends on the increase of β_0^n, i.e., the increase in n with GBD →VD change, though the nQ also increases by Al_2O_3 or SiO_2 addition. Therefore, the kinetic process of VD is faster than that of dominant GBD by the segregated dissolution of Al_2O_3 or SiO_2 at Y-TZP grain boundaries. Furthermore, the increase in β_0^n depends primarily on the increase in γ_S, which corresponds to the increase in $V_O^{\bullet\bullet}$. It is, therefore, explained that the sintering rate of 3YA is greater than that of 3YC because of the increase in $V_O^{\bullet\bullet}$ produced by dissolution of Al_2O_3.

5. Conclusions

In the present study, the effects of Al_2O_3 and SiO_2 addition on initial sintering of Y-TZP powder manufactured by the hydrolysis process were investigated. The following conclusions were obtained:

(1) The sintering rate of Y-TZP powder remarkably increased by a small amount of Al_2O_3 or SiO_2 addition, and the enhanced sintering effect by Al_2O_3 addition was greater than that by SiO_2 addition. Al_2O_3 or SiO_2 addition affected little the grain-growth process at the hold-time condition in the present sintering profiles.

(2) The nQ and β_0^n at the initial sintering stage were estimated by applying the sintering-rate equation to the CRH data. The diffusion mechanism changed from GBD to VD by Al_2O_3 or SiO_2 addition. Both nQ and β_0^n increased in the order of 3YA > 3YC > 3Y. It is, therefore, concluded that the sintering rate increases in the order of 3YA > 3YC > 3Y because the increase in β_0^n rather than nQ is predominant. This enhanced sintering mechanism is reasonably interpreted by the segregated dissolution of Al_2O_3 or SiO_2 at Y-TZP grain boundaries.

(3) The present analytical method derived based on the sintering kinetics at CRH is very useful for determination of the diffusion mechanism at the initial sintering stage of ceramic powders.

Acknowledgement

The author would like to express his sincere thanks to Professor Junichi Hojo, Kyushu University, for his valuable advice in this work.

References

1）W.S.Young and I.B.Cutler, *J.Am.Ceram.Soc.*, **53**(12), 659(1970)
2）J.Wang and R.Raj, *J.Am.Ceram.Soc.*, **73**(5), 1172(1990)
3）J.Wang and R.Raj, *J.Am.Ceram.Soc.*, **74**(8), 1959(1991)
4）K.Matsui, N.Ohmichi, M.Ohgai, N.Enomoto, and J.Hojo, *J.Am.Ceram.Soc.*, **88**(12), 3346(2005)
5）K.Matsui, K.Tanaka,, N.Enomoto, and J.Hojo, *J.Ceram.Soc.Jpn.*, **114**(9), 763(2006)
6）K.Matsui, T.Yamakawa, M.Uehara, N.Enomoto, and J.Hojo, *J.Am.Ceram.Soc.*, **91**(6), 1888(2008)
7）K.Matsui, A.Matsumoto, M.Uehara, N.Enomoto, and J.Hojo, *J.Am.Ceram.Soc.*, **90**(1), 44(2007)
8）K.Matsui, K.Tanaka, T.Yamakawa, M.Uehara, N.Enomoto, and J.Hojo, *J.Am.Ceram.Soc.*, **90**(2), 443(2007)
9）Y.Moriyoshi and W.Komatsu, *Yogyo-Kyokai-Shi*, **79**(10), 370(1971)
10）D.L.Johnson, *J.Appl.Phys.*, **40**(1), 192(1969)
11）Y.Moriyoshi and W.Komatsu, *J.Am.Ceram.Soc.*, **53**(12), 671(1970)
12）D.L.Johnson and I.B.Cutler, *J.Am.Ceram.Soc.*, **46**(11), 541(1963)
13）D.L.Johnson and I.B.Cutler, *J.Am.Ceram.Soc.*, **46**(11), 545(1963)
14）H.Su and D.L.Johnson, *J.Am.Ceram.Soc.*, **79**(12), 3211(1996).
15）Y.Ikuhara, Y.Nagai, T.Yamamoto, and T.Sakuma, *Interface Science*, **7**, 77(1999)
16）Y.Ikuhara, P.Thavorniti, and T.Sakuma, *Acta. Mater.*, **45**(12), 5275(1997)
17）J.Zhao, Y.Ikuhara, and T.Sakuma, *J.Am.Ceram. Soc.*, **81**(8), 2087(1998)

18) P.Thavorniti, Y.Ikuhara, and T.Sakuma, *J.Am. Ceram.Soc.*, **81**(11), 2927(1998).
19) T.Yamaguchi, *Ceramics Jpn.*, **19**(6), 520(1984)
20) Y.Ikuhara, T.Yamamoto, A.Kuwabara, H.Yoshida, and T.Sakuma, *Science and technology of advanced materials*, **2**, 411(2001)
21) Y.Sakka, Y.Oishi, and K.Ando, *J. Mater. Sci.*, **17**(11), 3101(1982)
22) Y.Sakka, Y.Oishi, K.Ando, and S.Morita, *J.Am. Ceram.Soc.*, **74**(10), 2610(1991).
23) H.Yanagita, K.Kawamoto, and M.Miyayama, " Kesshouchu deno Kakusan (Diffusion in Crystal) ";pp.125-29 in seramikkusu no kagaku (Chemistry of Ceramics), Edited by H.Yanagita. Maruzen Co., Ltd, Tokyo, Japan, 1996.

著　　者
氏名　松 井 光 二
Koji MATSUI
入社　昭和61年4月1日
所属　東京研究所
新材料・無機分野
主席研究員